$Ba_3Yb(BO_3)_3$ single crystals: Growth and spectroscopic characterization

R. Solé[a)]
Física i Cristal·lografia de Materials (FiCMA), Universitat Rovira i Virgili (URV), Campus Sescelades, E-43007 Tarragona, Catalunya, Spain

F. Güell
Enginyeria i Materials Electrònics (EME), Departament d'Electrònica, Universitat de Barcelona, E-08028 Barcelona, Catalunya, Spain

Jna. Gavaldà, M. Aguiló, and F. Díaz
Física i Cristal·lografia de Materials (FiCMA), Universitat Rovira i Virgili (URV), Campus Sescelades, E-43007 Tarragona, Catalunya, Spain

(Received 7 February 2008; accepted 13 June 2008)

We obtained $Ba_3Yb(BO_3)_3$ single crystals by the flux method with solutions of the BaB_2O_4–Na_2O–Yb_2O_3 system. The evolution of the cell parameters with temperature shows a slope change at temperatures near 873 K, which may indicate a phase transition that is not observed by changes appearing in the x-ray powder patterns or by differential thermal analysis (DTA). The evolution of the diffraction patterns with the temperature shows incongruent melting at temperatures higher than 1473 K. DTA indicates that there is incongruent melting and this process is irreversible. $Ba_3Yb(BO_3)_3$ has a wide transparency window from 247 to 3900 nm. We recorded optical absorption and emission spectra at room and low temperature, and we determined the splitting of Yb^{3+} ions. We used the reciprocity method to calculate the maximum emission cross section of 0.28×10^{-20} cm^2 at 966 nm. The calculated lifetime of Yb^{3+} in $Ba_3Yb(BO_3)_3$ is $\tau_{rad} = 2.62$ ms, while the measured lifetime is $\tau = 3.80$ ms.

I. INTRODUCTION

In recent years, borate single crystals have been arousing increasing interest because of their potential as nonlinear optical materials and laser hosts. Many articles have been published on crystal growth and the discovery of new nonlinear optical borate crystals that can incorporate laser-active ions in their matrix to create a self-doubling material.[1–8]

Recently, laser crystals containing Yb^{3+} ions have attracted greater interest because their simple electronic structure has only two energy levels, the ground level and an excited level, separated by energy of about 10,000 cm^{-1}. Thus, there is no excited-state absorption, nor upconversion processes, and their quantum defect is small.[9]

$Ba_3Yb(BO_3)_3$ is a new noncentrosymmetrical crystal with the space group $P6_3cm$ and cell parameters $a = b = 9.411(1)$ and $c = 17.481(5)$ Å.[10] Because of the high content of Yb^{3+} in $Ba_3Yb(BO_3)_3$ and the lack of a symmetry center, this phase could be interesting as self-doubling material.[11]

In the present work, we study the growth conditions of $Ba_3Yb(BO_3)_3$ crystals in the BaB_2O_4–Na_2O–Yb_2O_3 system. The thermal evolution of the crystals obtained is characterized by x-ray powder diffraction and by differential thermal analysis (DTA). The linear thermal expansion tensor is also obtained. The final aim of this study is to characterize the optical properties of these crystals by measuring of the optical absorption and emission at room temperature and low temperature and to confirm that they are good candidates for self-doubling material and the fabrication of thin-disk lasers.

II. EXPERIMENTAL DETAILS

A. $Ba_3Yb(BO_3)_3$ crystal growth

In the BaB_2O_4–Na_2O–Yb_2O_3 system, $Ba_3Yb(BO_3)_3$ crystallizes as a neighboring phase of BaB_2O_4, when the Yb_2O_3 in the solution is high enough.

The experiments were made in a cylindrical vertical furnace controlled by a Eurotherm controller/programmer type 903 P. The reagents used were $BaCO_3$, B_2O_3, and Na_2CO_3, with purity higher than 99% and Yb_2O_3 with a purity of

a)Address all correspondence to this author.
e-mail: rosam.sole@urv.cat
DOI: 10.1557/JMR.2008.0313

 © 2008 Materials Research Society

99.9%. The solution composition was BaB_2O_4/Yb_2O_3 = 92/8 and $(BaB_2O_4 + Yb_2O_3)/Na_2O$ = 83/17 in molar ratios.

The solutions, weighing about 25 g, were prepared in a 25-cm^3 platinum crucible and homogenized at 1273–1373 K for several hours. The axial temperature gradient in the solution was 12 $K \cdot cm^{-1}$, with the crucible bottom and wall hotter than the center of the solution surface. The saturation temperature was about 1153 K and was determined by observing the growth or dissolution of small single crystals (less than 0.5 mm in size) thrown through a hole in the lid, by increasing or decreasing the solution temperature in steps of 1 to 2 K. These crystals stayed in the center of the solution surface because of the surface tension, accompanied by a weak free convection. Subsequently, to provide samples for x-ray diffraction (XRD) analysis, optical observation and thermal and spectroscopic characterizations, a platinum wire was immersed in the solution so that crystals could grow on it and be easily removed from the solution. To obtain these crystals, the temperature of the solution was decreased from the determined saturation temperature at a rate of about 0.2–1 $K \cdot h^{-1}$ for about 10–20 h. The crystals were then removed from the solution and maintained just above its surface, while the furnace was cooled at a rate of 50 $K \cdot h^{-1}$ to room temperature to avoid cracks.

The crystalline phase was identified by observation with an optical reflection microscope and also by x-ray powder diffraction with a Siemens D-5000 diffractometer.

The chemical composition of the crystals was obtained by electron probe microanalysis (EPMA), with wavelength dispersive spectroscopy (WDS), using a Cameca SX 50. Corrections for dead time, background, and matrix effect were carried out using the Pouchou and Pichoir (PAP) procedure.[12]

B. Thermal study of $Ba_3Yb(BO_3)_3$

X-ray powder diffraction analysis of $Ba_3Yb(BO_3)_3$ was made at different temperatures, with the same diffractometer used for identification of the phases, and now equipped with an Anton-Paar HTK10 high temperature chamber and scintillation counter as detector. The crystalline powder was placed on a platinum holder and the diffraction data for cell parameters calculation were obtained at temperatures between 298 and 1373 K, with 2θ = 9.30 – 70.11°, ss = 0.030°, st = 5 s, and a delay of 300 s before each measurement. The temperature was increased at a rate of 5 $K \cdot s^{-1}$. The external standard used was Si SMR 640b. These data were used to calculate the cell parameters, as a function of the temperature, using the Fullprof program.[13] The linear thermal expansion coefficients for every crystallographic direction between room temperature and 873 K were obtained from these parameters as $\alpha = (\Delta L/\Delta T)/L$, where ΔL is the change in the cell parameter corresponding to the given crystallographic direction, when the temperature is changed in ΔT and L is the parameter at 298 K.

The phase transitions of $Ba_3Yb(BO_3)_3$, with the temperature, were studied by x-ray powder diffraction and differential thermal analysis (DTA). In this case, the x-ray powder diffraction analysis was made at several temperatures using the above mentioned high temperature chamber together with the diffractometer and a Braun position sensitive detector (PSD). The measurements were made at 298, 973, 1073, 1173, 1223, 1273, 1323, 1373, 1423, 1473, 1503, 1523, and 1543, as shown in Fig. 1, with 2θ = 10–70°, ss = 0.020°, and the measuring time per degree was 10 s. Between room temperature and 973 K, the temperature was increased at a rate of 5 $K \cdot s^{-1}$; between 973 K and 1173 K the rate was 1 $K \cdot s^{-1}$, and between 1173 K and 1543 K the temperature was increased at 0.2 $K \cdot s^{-1}$.

DTA and thermogravimetric analysis (TGA) of $Ba_3Yb(BO_3)_3$ were carried out using simultaneous differential techniques equipment (SDT 2960) from TA Instruments. The temperature calibration of the equipment was made using standards with different melting temperatures such as Zn, Au, and Ni. The samples were placed in platinum cups and calcined Al_2O_3 powder was used as a reference, while an argon flux of 90 cm^3/min was maintained throughout the experiments. To study the possible phase transitions and melting temperature of this material, the temperature of the furnace was increased at a rate of 10 $K \cdot h^{-1}$ to 1543 K and then cooled to room temperature.

C. Spectroscopic characterization

Because of the high content of Yb in $Ba_3Yb(BO_3)_3$, it may be of interest in laser emission. Furthermore, because it has no center of symmetry, it could have properties that

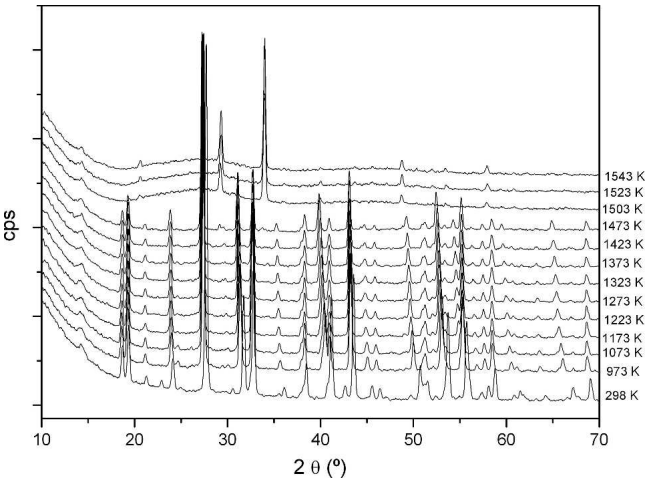

FIG. 1. Evolution of the $Ba_3Yb(BO_3)_3$ diffractograms with the temperature from room temperature to 1543 K.

are interesting for second-harmonic generation (SHG). The SHG of these crystals has already been studied in the literature and, depending on the particle size,[14] can be up to six times higher than the value for quartz.[10] However, the potentiality of this stoichiometric crystal for laser emission has not been studied yet. In the literature, the laser emission of several crystals of this family has been demonstrated only for low levels of Yb doping.[15,16] Thus, optical absorption and emission spectra of $Ba_3Yb(BO_3)_3$ have been carried out here in an attempt to contribute to the optical characterization of this material.

The transparency window of $Ba_3Yb(BO_3)_3$ was obtained with a Varian CARY 500 scan spectrophotometer in the range up to 3000 nm, and with a Fourier transform infrared spectroscopy (FTIR) Midac Prospect spectrophotometer from 3000 nm to the IR cutoff. The ultraviolet (UV) and IR cutoffs were obtained by considering the $1/e$ factor: that is to say, the UV (IR) cutoff is the wavelength at which the transmission is less than the maximum divided by the e number.

Optical absorption spectra were measured with the Varian CARY 500 scan spectrophotometer, which was used to obtain the transparency window. Cryogenic temperatures at 6 K were achieved with a Leybold RDK 6-320 closed cycle helium cryostat. This phase grows as very thin crystals; therefore, we used as-grown crystals (plates perpendicular to the c direction) for these measurements, and there was no need for cutting and polishing in thicker crystals. The sample is 0.21 mm thick, and the ytterbium concentration is 44.96×10^{20} atoms/cm^3.

Emission spectra were obtained with an optical parametrical oscillator, VEGA 100, pumped by the third harmonic of a Q-switched Nd^{3+}:YAG laser (pulse duration: 7 ns, repetition rate: 10 Hz) SAGA 120 from B.M. Industries. Fluorescence was dispersed through a HR460 Jobin Yvon-Spex monochromator and detected by a R5509-72 Hamamatsu photomultiplier. The signal was analyzed with a Perkin Elmer 7265DSP lock-in amplifier. Time decay curves were recorded using a Tektronix TDS-714 digital oscilloscope. For low temperature emission measurements, the samples were mounted on a closed cycle helium cryostat Oxford CCC1104.

III. RESULTS AND DISCUSSION

A. $Ba_3Yb(BO_3)_3$ crystal growth

The crystals obtained to be used for x-ray analysis, and thermal and spectroscopic characterization had the shape of hexagonal plates, with the c direction perpendicular to the plates. In the center, at the beginning of the crystal growth, the crystals generally had more defects, such as solvent inclusions, while on the periphery they were mainly transparent. These crystals tend to grow very thinly across the surface of the solution. A cleavage plane was also observed perpendicular to the c direction, which contributed to making thinner crystals. In the transparent part, they were generally less than 1 mm thick.

B. Thermal study of $Ba_3Yb(BO_3)_3$

$Ba_3Yb(BO_3)_3$ crystallizes in the hexagonal system with the space group $P6_3cm$, with $a = b = 9.411(1)$ and $c = 17.481(5)$ Å.[10] The change of these unit cell parameters with the temperature was calculated from x-ray powder diffraction data and the Fulproof program. Figure 2 shows the thermal dependence of the normalized cell parameters, $(L–L_{298})/L_{298}$, where L is the a or c cell parameter and L_{298} is the a or c unit cell parameter at a temperature of 298 K. Figure 2 also shows the behavior between each of the normalized cell parameters and the temperature is linear to about 873 K. At a temperature close to 873 K, a change in the evolution of the cell parameters with the temperature (slope change) could indicate a phase transition. This agrees with the literature, where the second harmonic generation properties were lost at a similar temperature (slightly higher), 913–943 K, indicating a phase transition to a centrosymmetric phase.[10,17] Nevertheless, this possible phase transition could not be detected by the XRD patterns obtained.

The thermal expansion tensor related with a material that crystallizes in the hexagonal system, is diagonal, and $\alpha_{11} = \alpha_{22} \neq \alpha_{33}$. These values are obtained from the unit cell parameters thermal change by the expression $\alpha_{ii} = (1/L_i)[(\partial L_i)/(\partial T)]$. The linear behavior of the $(L–L_{298})/L_{298}$, with the temperature up to about 873 K indicates that the thermal expansion coefficients do not change with the temperature in this range and can be obtained from the slope of the linear fits from room temperature to 873 K. The linear thermal expansion tensor in the crystallophysical orthogonal system (X_1 // a, X_2 // b^* and

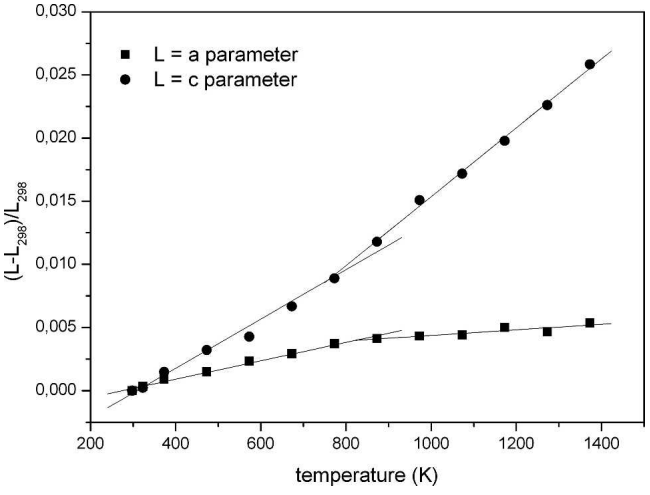

FIG. 2. Evolution of the normalized cell parameters with the temperature.

X_3 // c, with $b^* = c \times a$, is a vector of the reciprocal space) between room temperature and 873 K is

$$(\alpha_{ij}) = \begin{pmatrix} 7.3 & & \\ & 7.3 & \\ & & 19.5 \end{pmatrix} \times 10^{-6}\ \mathrm{K}^{-1} \quad .$$

As can be seen above, there is an important anisotropy between the directions in the *a-b* plain and the *c* direction.

From the evolution of the diffractograms with the temperature (Fig. 1) between room temperature and 1473 K, any change in the diffraction pattern that could indicate a phase change is observed. At 1503 K, however, there is a partial melting, accompanied by the crystallization of a new phase, the Yb_2O_3, while the $Ba_3Yb(BO_3)_3$ disappears. The Yb_2O_3 is maintained and its peaks intensify at least up to 1543 K.

DTA was made on $Ba_3Yb(BO_3)_3$ and the results are shown in Fig. 3. In the heating process two peaks are observed, which means there is an incongruent melting at 1514 K, before the melting at a temperature of 1530 K. According to XRD measurements, at 1503 K there is an incongruent melting and Yb_2O_3 crystallizes. This phase is maintained at least up to 1543 K. The differences between DTA and x-ray measurements could be explained by the temperature differences between the control thermocouple and the temperature of the sample studied in XRD. These results partially agree with the literature, where melting temperatures of 1489 K[18] and 1523 K[10] have been found, although no phase transition before the melting point has been detected by DTA in the literature.[10,18] According to the literature, a type I phase transition would be expected at 943 K in the heating process, and would be detected by a dramatic decrease in the SHG at this temperature.[10] We have not observed this phase transition either by DTA-TGA measurements or by direct x-ray powder diffraction. However a change in the slope of the evolution of the normalized cell parameters with the temperature was observed at a temperature of about 873 K, which could be related to this phase transition.

C. Spectroscopic characterization

Figure 4 shows the measured transmission of $Ba_3Yb(BO_3)_3$ for a sample thickness of 0.21 mm, and the range of transparency is wide. The UV cutoff wavelength, calculated as $1/e$ of the maximum value, is around 247 nm (40486 cm^{-1}) and the transparency extends to 3900 nm (2563 cm^{-1}). The absorption band near 960 nm will be analyzed below.

Optical absorption spectra of $Ba_3Yb(BO_3)_3$ at room temperature and 6 K were obtained using unpolarized light. Because of the symmetry of this phase, space group $P6_3cm$ using an as-grown crystal with plate shape along a plane perpendicular to *c* direction, in this plane, indicates the different crystallographic directions are equivalent. Figure 5(a) shows the measured absorption cross-sections (σ_a) for the $^2F_{7/2} \rightarrow {}^2F_{5/2}$ transition obtained at room temperature (solid line). The maximum absorption cross section is 0.25×10^{-20} cm^2 at 966 nm. Figure 5(b) shows the splitting of this unique manifold of Yb^{3+} ions obtained at 6 K. The peaks observed are located at 908.8, 965.6, and 968.2 nm and correspond to the electronic transitions $^2F_{7/2}(0) \rightarrow {}^2F_{5/2}(2')$, $^2F_{7/2}(0) \rightarrow {}^2F_{5/2}(1')$, and $^2F_{7/2}(0) \rightarrow {}^2F_{5/2}(0')$, respectively. We labeled the *n* Stark levels, increasing in energy from 0 to *n*, *n'* for the upper level and *n* for the lower level. The Stark sublevels of the excited state $^2F_{5/2}$ are located at 11004, 10356, and 10328 cm^{-1}, respectively.

One of the most important parameters that influence the laser performance of a material is the stimulated emission cross-section (σ_e). We calculated the emission cross-section spectra of the $^2F_{5/2} \rightarrow {}^2F_{7/2}$ transition by a

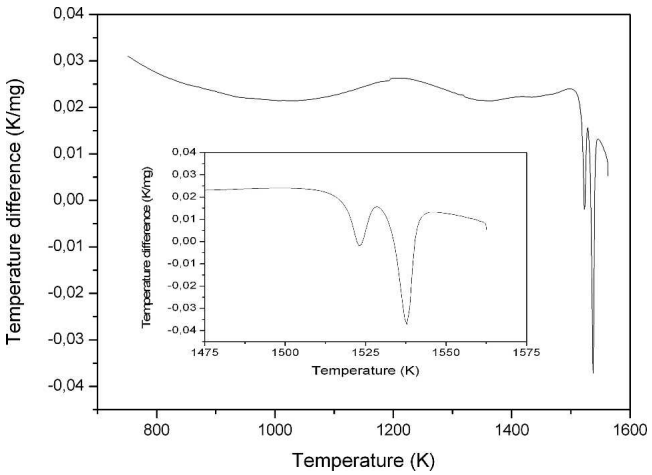

FIG. 3. DTA of $Ba_3Yb(BO_3)_3$.

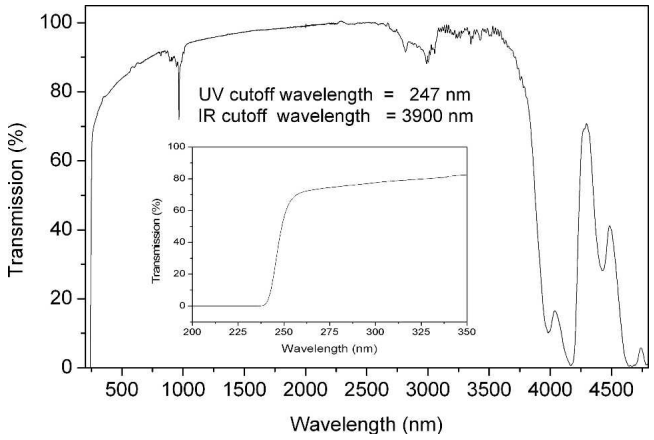

FIG. 4. Optical transparency window of a 0.21-mm-thin sample of $Ba_3Yb(BO_3)_3$ at room temperature. The inset shows a detail of the UV cutoff.

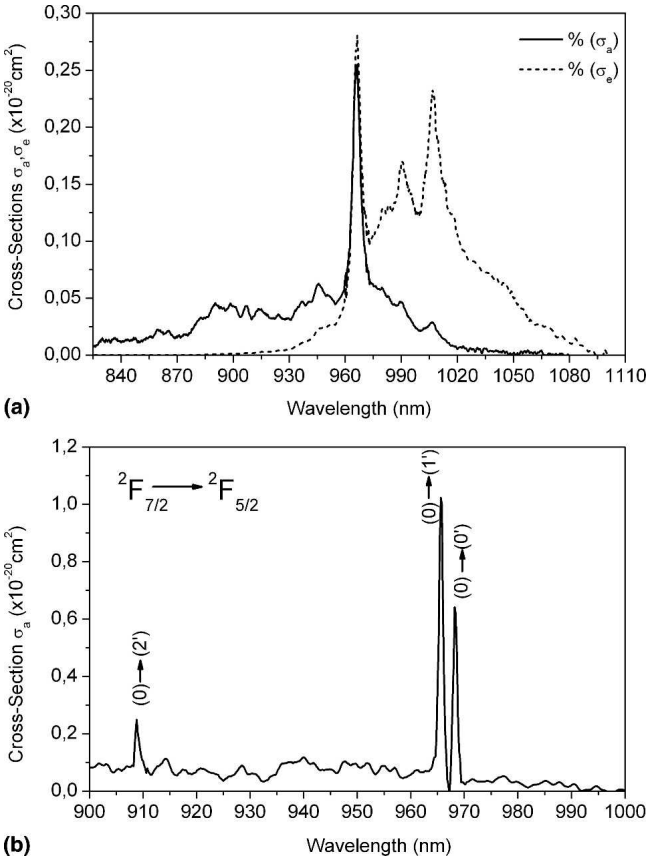

FIG. 5. (a) Absorption cross-sections σ_a corresponding to the $^2F_{7/2} \rightarrow {}^2F_{5/2}$ transition (solid line) and emission cross-sections σ_e (dashed line) calculated by the reciprocity method of $Ba_3Yb(BO_3)_3$ at room temperature. (b) Optical absorption spectrum of $Ba_3Yb(BO_3)_3$ at 6 K.

so-called reciprocity method (RM).[19] The emission cross-section (σ_e) is calculated from the absorption cross-section (σ_a) and the splitting of the energy levels using the following equation:

$$\sigma_e(\nu) = \sigma_a(\nu)\frac{Z_l}{Z_u}\exp\left[\frac{(E_{ZL} - h\nu)}{k_B T}\right] \quad , \qquad (1)$$

where Z_l and Z_u are the partition functions, and E_{zl} is the zero-line or energy separation between the lowest energy sublevels of the ground state (lower) and the first excited state (upper), respectively, h and K_B are the Planck and Boltzmann constants, respectively, and T is the temperature in K. The partition functions are calculated from:

$$Z = \sum_k d_k \exp\left[\frac{-E_k}{k_B T}\right] \quad , \qquad (2)$$

where d_k and the E_k are the degeneracies and the energies, respectively, of each sublevel of the upper and lower energy levels involved. In our case, the ratio Z_l/Z_u was 1.25 and E_{zl} was 10328 cm^{-1}. Figure 5(a) shows the calculated emission cross sections for the $^2F_{5/2} \rightarrow {}^2F_{7/2}$ transition at room temperature in the 900–1100 nm range (dotted line). The maximum emission cross section is 0.28×10^{-20} cm^2 at 966 nm. These absorption and emission cross-sections spectra will be useful for designing and modeling CW and pulsed lasers.

For the luminescence studies, we pumped the sample at 940 nm. The emission spectra of $Ba_3Yb(BO_3)_3$ at room temperature and 10 K are shown in Fig. 6. At 10 K, we observed seven peaks located at 965.6, 968.2, 991.2, 993.9, 1006, 1009, and 1028 nm, which correspond to the electronic transitions $^2F_{5/2}(1') \rightarrow {}^2F_{7/2}(0)$, $^2F_{5/2}(0') \rightarrow {}^2F_{7/2}(0)$, $^2F_{5/2}(1') \rightarrow {}^2F_{7/2}(1)$, $^2F_{5/2}(0') \rightarrow {}^2F_{7/2}(1)$, $^2F_{5/2}(1') \rightarrow {}^2F_{7/2}(2)$, $^2F_{5/2}(0') \rightarrow {}^2F_{7/2}(2)$, and $^2F_{5/2}(0') \rightarrow {}^2F_{7/2}(3)$, respectively. The Stark sublevels of the ground state $^2F_{7/2}$ are located at 0, 267, 416, and 600 cm^{-1}, respectively. In summary, the Stark splitting of the energy levels of Yb^{3+} ions obtained in the $Ba_3Yb(BO_3)_3$ host is pictured in the inset of Fig. 6.

The $^2F_{5/2} \rightarrow {}^2F_{7/2}$ transition corresponds to a quasi-three-level laser scheme in which the lower level is thermally populated at RT. This results in considerable reabsorption and increased threshold for laser operation. Reducing reabsorption and maintaining efficient absorption of the pump light is one of the key issues in the design of ytterbium-doped laser systems on this transition. The reabsorption processes of the 1-μm emission by resonant transitions occur when the overlapping of absorption and emission is important. As a first approximation, the threshold for light amplification is reached when the emitted light counterbalances the absorption losses. If β is the population inversion rate, this condition can be described as $\sigma_{gain} = \beta \cdot \sigma_e - (1 - \beta) \cdot \sigma_a$, where σ_{gain} is the effective emission cross section. Figure 7 shows this condition in the 960–1100 nm spectral region for the $^2F_{5/2} \rightarrow {}^2F_{7/2}$ transition. The population inversion rate needed to achieve amplification is expected to be higher than 0.05. For a population inversion level of 0.2,

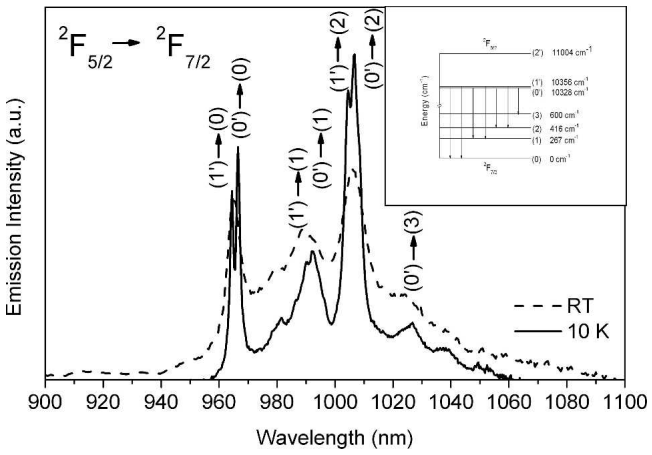

FIG. 6. Emission spectra of $Ba_3Yb(BO_3)_3$ obtained at room temperature (dashed line) and 10 K (solid line). The inset shows the Stark splitting of the energy levels of Yb^{3+} ions in the $Ba_3Yb(BO_3)_3$ host.

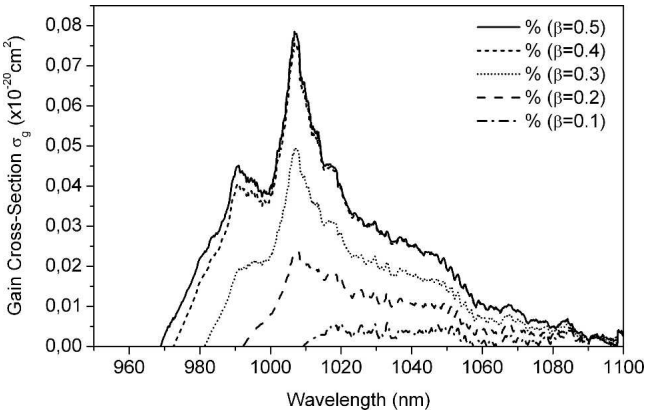

FIG. 7. Gain cross sections of the 1-μm emission at RT at several inversion population rates.

the gain is produced in the 992–1100 nm range. The highest energy limit of this interval increased when the population inversion level was increased, reaching as high as 969 nm for a population inversion level of 0.5. For this level, the maximum gain cross-section value was 0.08×10^{-20} cm^2 at 1007 nm. At this point, we expect to find light amplification in future laser experiments for this emission.

From the emission cross-sections σ_e (ν), the radiative lifetime τ_{rad} can be estimated using the Füchtbauer-Ladenburg equation.[20] The error originating from the thermal distribution of the population in the ground state $^2F_{7/2}$ at room temperature when calculating σ_a (ν) can be suppressed by integrating the corresponding equation over the frequency[21]

$$\frac{1}{\tau_{rad}} = 8\pi n^2 \int \frac{\sigma_e(\nu)}{\lambda^2} d\nu \quad , \tag{3}$$

where n is the refraction index, λ the wavelength, and ν the frequency. Using the σ_e (ν) dependence calculated by the reciprocity method [Fig. 5(a)], we obtain τ_{rad} = 2.62 ms at room temperature, in comparison to the measured value of τ = 3.8 ms. These values are comparable with the value obtained in the literature for a compound of the same family.[22] To compare the potential laser capabilities of different media, it is better to use the characteristic value $\sigma_e \times \tau$ [the laser threshold is proportional to $(\sigma_e \times \tau)^{-1}$]. This value is 1.06×10^{-20} cm^2·ms for $Ba_3Yb(BO_3)_3$.

IV. CONCLUSIONS

In this study, we obtained $Ba_3Yb(BO_3)_3$ crystals suitable for x-ray powder diffraction and thermal and spectroscopic characterization. The thermal study of this phase shows a change in the slope of the evolution of cell parameters with the temperature at about 873 K. This could be related to a phase transition to a centrosymmetric phase. This possible phase transition could not be detected by the x-ray patterns obtained. The thermal expansion coefficients of this phase up to 873 K have also been calculated, and they show a significant anisotropy between the *a-b* plain and the *c* direction. The evolution of the diffractograms with the temperature show that up to 1473 K any phase transition could be detected by changes in the diffraction patterns obtained, while at about 1503 K there is a decomposition accompanied by partial melting. From the DTA-TGA study, we observed a phase transition at 1514 K and melting at 1530 K, showing that $Ba_3Yb(BO_3)_3$ melts incongruently.

The absorption spectrum at room temperature has the only manifold of Yb^{3+} corresponding to the transition $^2F_{7/2} \rightarrow {}^2F_{5/2}$, centered at 966 nm. Using the absorption spectrum at 6 K, we determined the splitting of the $^2F_{5/2}$ excited state. Using the 10 K emission spectrum, we determined the splitting of the $^2F_{7/2}$ ground state. We calculated the stimulated emission cross section using the reciprocity method. The maximum emission cross section is 0.28×10^{-20} cm^2 at 966.4 nm. Therefore, we were able to calculate the optical gain for several population inversion rates and determine the spectral region in which light can be amplified for future laser experiments using this material. From the gain wavelength, we found a tunability range >120 nm for the $^2F_{5/2} \rightarrow {}^2F_{7/2}$ transition. The lifetime of Yb^{3+} in $Ba_3Yb(BO_3)_3$ calculated from the emission cross-sections spectrum is 2.62 ms, while the measured value is 3.8 ms. The long lifetime of the $^2F_{5/2}$ energy level shows that population inversion is expected to be easy. This is needed to generate laser radiation.

ACKNOWLEDGMENTS

This work was supported by the Spanish government under Projects MAT-05-06354-C03-02, MAT-04-20471-E, and CIT-020400-2005-14 and the Catalan government under Project 2005SGR658.

REFERENCES

1. F.Y. Zavartsev, S.A. Koutovoi, V.V. Voronov, V.V. Panyutin, A.I. Zagumennyi, and I.A. Shcherbakov: Phenomenon of metastable liquation during BiB_3O_6 crystallization. *J. Cryst. Growth* **275,** 637 (2005).
2. N.I. Leonyuk, E.V. Koporulina, V.V. Maltsev, J. Li, H.J. Zhang, J.X. Zhang, and J.Y. Wang: Growth and characterization of $(Tm,Y)Al_3(BO_3)_4$ and $(Yb,Y)Al_3(BO_3)_4$ crystals. *J. Cryst. Growth* **277,** 252 (2005).
3. D. Zhao, Z. Hu, Z. Lin, and G. Wang: Growth and spectral properties of Er^{3+}/Yb^{3+}-codoped $Sr_3Y(BO_3)_3$ crystal. *J. Cryst. Growth* **277,** 401 (2005).
4. M. Nishioka, A. Kanoh, M. Yoshimura, Y. Mori, and T. Sasaki: Growth of $CsLiB_6O_{10}$ crystals with high laser damage tolerance. *J. Cryst. Growth* **279,** 76 (2005).
5. D. Eimerl, L. Davis, S. Velsko, E.K. Graham, and A. Zalkin:

Optical, mechanical, and thermal properties of barium borate. *J. Appl. Phys.* **62,** 1968 (1987).
6. D.N. Nikogosyan: Beta-barium borate (BBO): A review of its properties and applications. *Appl. Phys. A: Mater. Sci. Process.* **52,** 359 (1991).
7. T. Ding-Yuan: Nonlinear optical BBO crystals: Growth, properties and applications. *Chin. J. Struct. Chem.* **19,** 112 (2000).
8. R. Solé, V. Nikolov, M.C. Pujol, Jna. Gavaldà, X. Ruiz, J. Massons, M. Aguiló, and F. Díaz: Stabilization of β-BaB_2O_4 in the system BaB_2O_4–Na_2O–Nd_2O_3. *J. Cryst. Growth* **207,** 104 (1999).
9. X. Zou and H. Tortani: Evaluation of spectroscopic properties of Yb^{3+} doped glasses. *Phys. Rev. B* **52,** 15889 (1995).
10. T.N. Khamaganova, N.M. Kuperman, and Zh.G. Bazarova: The double borates $Ba_3Ln(BO_3)_3$, Ln = La–Lu. *J. Solid State Chem.* **145,** 33 (1999).
11. C. Stewen, K. Contag, M. Larionov, A. Giesen, and H. Hügel: A 1 Kw CW thin disc laser. *IEEE J. Sel. Top. Quantum Electron.* **6,** 650 (2000).
12. J.L. Pouchou and F. Pichoir: A new model for quantitative x-ray microanalysis. 1. Application to the analysis of homogeneous samples. *Rech. Aerosp.* **3,** 13 (1984).
13. J. Rodríguez-Carvajal: Recent advances in magnetic structure determination by neutron powder diffraction. *Physica B* **192,** 55 (1993).
14. S.Yu. Stefanovich and T.N. Khamaganova: Nonlinear optical properties of $Ba_3R(BO_3)_3$ (R = Y, Ho–Lu) polar crystals. *Inorg. Mater.* **38,** 66 (2002).
15. P.H. Haumesser, R. Gaumé, B. Viana, and D. Vivien: Determination of laser parameters of ytterbium-doped oxide crystalline materials. *J. Opt. Soc. Am. B* **19,** 2365 (2002).
16. R. Gaumé, P.H. Haumesser, E. Antic-Fidancev, P. Porcher, B. Viana, and D. Vivien: Crystal field calculations of Yb^{3+}-doped double borate crystals for laser applications. *J. Alloys Compd.* **341,** 160 (2002).
17. J.J. Carvajal, R. Solé, Jna. Gavaldà, J. Massons, F. Díaz, and M. Aguiló: Phase transitions in RbTiOPO4-doped with niobium. *Chem. Mater.* **15,** 2730 (2004).
18. J.R. Cox, D.A. Keszler, and J. Huang: The layered borates $Ba_3M(BO_3)_3$ (M = Dy, Ho, Y, Er, Tm, Yb, Lu and Sc). *Chem. Mater.* **6,** 2008 (1994).
19. D.E. McCumber: Einstein relations connecting broadband emission and absorption spectra. *Phys. Rev. A* **136,** 954 (1964).
20. L.D. Deloach, S.A. Payne, L.L. Chase, L.K. Smith, W.L. Kway, and W.F. Krupke: Evaluation of absorption and emission properties of Yb^{3+} doped crystals for laser applications. *IEEE J. Quantum Electron.* **29,** 1179 (1993).
21. F.D. Patel, E.C. Honea, J. Speth, S.A. Payne, R. Hutcheson, and R. Equal: Laser demonstration of $Yb_3Al_5O_{12}$ (YbAG) and materials properties of highly doped Yb:YAG. *IEEE J. Quantum Electron.* **37,** 135 (2001).
22. S.K. Pan, S. Lu, D.Z. Ding, G.H. Ren, W.D. Zhang, G.F. Wang, and J.G. Pan: Growth and spectral properties of Yb^{3+}-doped $Ba_3Gd(BO_3)_3$ crystal. *Chin. J. Struct. Chem.* **26,** 1153 (2007).